Model testing to reveal the mechanics of pipeline ploughing in mega-ripples

Hatherley, Andrew; Bransby, Mark Fraser; Lauder, Keith; Brown, Michael

Published in:
Proceedings Of The Eighteenth (2008) International Offshore And Polar Engineering Conference, Vol 2

Publication date:
2008

Document Version
Publisher's PDF, also known as Version of record

Proceedings of the Eighteenth (2008) International Offshore and Polar Engineering Conference
Vancouver, BC, Canada, July 6-11, 2008

ISBN 978-1-880653-70-8 (Set); ISBN 1-880653-68-0 (Set)

Model Testing to Reveal the Mechanics of Pipeline Ploughing in Mega-Ripples

Andrew Hatherley, Mark Fraser Bransby, Keith Lauder, Michael Brown
Civil Engineering, University of Dundee
Dundee, Angus, UK

ABSTRACT

The paper reports an investigation of offshore pipeline plough behaviour in regions of seabed mega-ripples. Of particular interest is how the drag force and trench geometry are affected. Information was achieved by conducting a series of reduced scale laboratory tests using a 1/50th scale model plough. A parametric study revealed that the wavelength and amplitude of the sand waves with respect to the plough length are the key parameters influencing plough-sand wave interaction. The results have implications for offshore pipeline installers when encountering these geo-hazards.

KEY WORDS: pipeline plough; seabed; mega-ripples; trench depth; drag forces.

INTRODUCTION

An offshore pipeline plough is used to cut a trench in the seabed in which a pipeline is placed and backfilled (Palmer, 1979). The important aspects of plough performance are the velocity at which the plough can be dragged and the cover depth that is achieved (Cathie & Wintgens, 2001). Without sufficient cover depth, pipelines may be vulnerable to upheaval bucking, requiring expensive remedial rock-dumping or multiple plough passes may be required to achieve the required depth. The velocity of the plough depends on the drag force-velocity relationship (Palmer, 1999; Brown et al., 2006) for the plough as offshore vessels pull at a relatively constant drag force. If the required soil resistances are larger, the plough will have to go more slowly, resulting in potential cost and time over-runs. All prediction models, to date, concern only the performance of ploughs in uniform, level sea beds and use empirical relationships (e.g. Reese & Grinstead, 1986; Cathie & Wintgens, 2001).

This paper aims to investigate the performance of a plough in zones of mega-ripples. These are areas of seabed which contain regular surface features (Allen, 2000; Morrow & Larkin, 2007). Allan (2000) described these features as ripples, megaripples, sand waves depending on their size. The two main geometric parameters of the waves are their wavelength, L and their amplitude, h (measured peak to trough). The smaller features are particularly problematic as they undergo continuous changes. Hence, the exact morphology of the mega-ripples may change between the time when a pipeline route is surveyed and the time of pipeline installation and so they may not be able to be avoided.

In order to investigate plough performance in areas of mega-ripples a series of laboratory model tests were conducted. These utilized a 1/50th scale model plough as described by Bransby et al. (2005). The tests are used to reveal the interaction of the model plough with sand waves with a range of amplitudes and wavelengths and concentrate particularly on the achieved trench depth and the plough tow forces required in the different conditions. The experimental methods are reported first, before the results are presented and discussed.

EXPERIMENTAL METHODS

Introduction

A series of laboratory tests were conducted using a 1/50th scale model plough using testing apparatus previously described by Brown et al. (2006). All tests were carried out in loose, dry sand but for different seabed morphologies. Dry sand was used to isolate the 'static' (i.e. without rate effects) terms of the plough force relationships as drained soil response would have been provoked. A much larger parametric array of tests would be required to study also the effect of tow rate on the plough-wave interaction and this should be performed in the future.

Details of the series of tests is given in Table 1. Three wavelengths and three different amplitude ratios (h/L) were investigated. The three wavelengths selected were 1000 mm, 500 mm and 300 mm. These correspond to full-scale wavelengths, L = 50 m, 25 m and 15 m and so correspond to large mega-ripples or small sand waves (Gass et al, 1984). The model plough was 344 mm long and so these wavelengths correspond to 2.91, 1.45 and 0.87 times the plough length.

The waveform created in the sand model took the form of a cosine wave:

$$y = y_o + \frac{h}{2}\left(1 - \cos\frac{2\pi}{L}x\right), \qquad (1)$$

where y is the height of soil, y_o is the height of a flat bed without waves, x is the horizontal position and $h/2$ is the amplitude. Wave geometries were selected with constant amplitude to wavelength ratios (h/L) to ensure that they were self-similar. Consequently, all tests with h/L = 0.1 had a bed-form with a maximum slope inclination of 17.4^o

Table 1. The test series.

Test identifier	Number of waves	Wavelength L, mm	Amplitude (h/L)
0	0	-	0
1_0.1	1	1000	0.1
2_0.2	2	500	0.2
2_0.1	2	500	0.1
2_0.05	2	500	0.05
3_0.1	3	333	0.1
3_0.05	3	333	0.05

to the horizontal. The equivalent maximum angles were 32° and 8.9° for h/L = 0.2 and 0.05 respectively.

Apparatus

The series of tests were conducted using a 1/50th scale model plough. This has been used in previously reported tests (Bransby et al., 2005; Brown et al., 2006) designed to investigate plough rate effects in flat soil beds. The model has all linear dimensions reduced by a factor of 50 compared to a typical real plough and the mass reduced by a factor of 50^3. Further details are given by Bransby et al. (2005).

A general schematic of the testing apparatus is shown in Figure 1. The soil container was of length 2 m, breadth 0.5 m and allowed soil depths up to 0.4 m to be placed. One large front face of the box was constructed from Perspex to allow easier visualization of the plough behaviour.

Actuation was achieved using a high torque 12 V DC motor connected to a winch of 40 mm diameter. This pulled a wire which was connected though a pulley to the plough (Fig. 1). The displacement rate was controlled by varying the voltage input to the DC motor, but for the dry sand tests reported here, all tests were conducted at 10-11 mm/sec and soil behaviour will be independent of rate selected.

A load cell of capacity 50 N was placed on the plough, positioned so that it measured the tensile force in the tow wire. During calibration tests, a draw wire transducer measured the horizontal displacement of the plough. This was used to fix the displacement rate for the tests. As the plough moved through the sand waves (after first going through transition) the plough rotated in the plane shown in the elevation in Figure 1. This inclination was measured with a clinometer (accurate to 0.1°) which was calibrated to give zero readings when horizontal. The clinometer was calibrated so that a positive rotation represented the back of the plough being lower than the front (aft-pitching). The instruments were logged throughout each test and stored as ASCII data. In addition to the above data collection, some tests were digitally photographed with time-lapse photography through the Perspex front-face and others were digitally videoed.

Soil preparation

Dry, fine Congleton sand was used in the study. This is a uniform (C_u = 1.5), fine (d_{60} = 0.15 mm) silica sand. It has a critical state friction angle, ϕ'_{crit} = 31° and ρ_{max} = 1986 kg/m^3 and ρ_{min} = 1461 kg/m^3 (Brown et al., 2006).

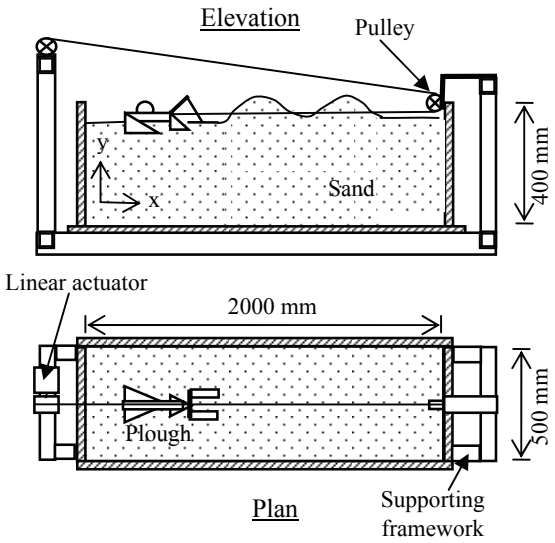

Fig. 1. Schematic showing general laboratory apparatus.

Sand beds were prepared by first 'stirring' the soil. This should have ensured that it reached a uniform critical state condition ($D_r \approx 20\%$). Then, the surface was scraped to the appropriate bed-form. This was achieved using a flat plate which was supported on rails from above. These rails were cut from plywood to form the appropriate sand surface profiles as detailed in Eq. 1 and Table 1. The soil surface profile was measured in all tests so that it could be compared to the final profile and so the accuracy of the modeled waves could be checked.

In all tests, the mega-ripples/sandwaves extended for approximately 1000 mm along the box. This meant that there was one sand wave when L = 1000 mm, two sand waves when L = 500 mm and three when L = 300 mm. To the left (in Fig. 1) of the wave zone there was a flat section designed to allow the plough to go transition to a steady-state condition before encountering the waves. The flat zone after the last wave (Fig. 1) could not be used as the tow-wire pulling angle to the horizontal increased as the pulley was reached, invalidating the results.

Testing procedure

After preparation of the sand sample, the plough was placed on the sand surface in the correct orientation to be pulled. The remainder of the apparatus (Fig. 1) was assembled and the data logging system was connected. The test was started by powering the DC motor and the plough was pulled through the sample continuously until it was approximately 300 mm from the right hand edge of the sample. A photograph of a test in progress is shown in Figure 2.

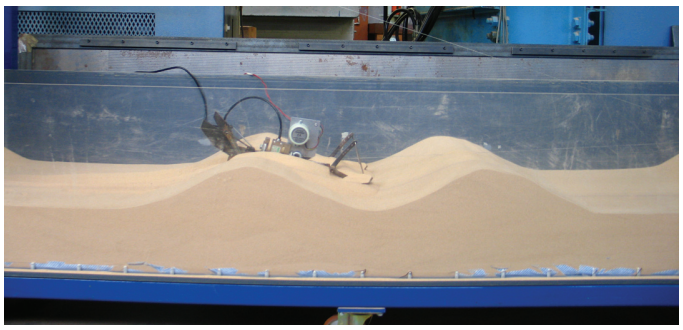

Fig. 2. Photograph of test under-way : Test 2_0.2.

Following testing, measurements were taken of the trenched profile along the centre-line of the trench (i.e. showing variation of y with x) and the height of the soil surface was measured at several points along the box (to show variation of y with out of plane position, z). This allowed measurement of the achieved trench depth (by comparing with the soil heights before trenching) and of the spoil heap sizes respectively. In some additional mechanism tests, the plough was pulled with displacement increments and measurements were taken when the plough had displaced different distances.

RESULTS

Flat soil bed

The plough performance in a flat soil bed of loose, dry sand was investigated first so that comparisons could be made with later tests and so that parameters for use in a tow force prediction model (Reese and Grinstead, 1986) could be verified. Several tests were first conducted to investigate the plough set-up to achieve different trenching depths and to investigate the force-trench depth relationship (Lauder et al. 2008). The plough skids were set so that the achieved trench depth was 32 mm in the flat soil sample. This is equivalent to a full-scale depth of 1.6 m which is typical offshore.

Figure 3 shows results for the first test. The solid triangles mark the tow force – displacement relationship. The plough starts with the tip of the skid 400 mm from the left of the edge of the box (i.e. at x = 400 mm) and the test finishes when x = 1798 mm. Figure 3 shows that on starting to displace the plough there is a gradual increase of tow force, 'transition', until a steady-state tow force is achieved. Transition is complete after a displacement of about 500 mm (i.e. at x = 900 in Fig. 2), after which there is an approximately constant tow force of 16 N, albeit subject to experimental 'noise'. A reduction in force starts to show when x > 1400 mm which is due to the angle of cable pull to the horizontal increasing as the box edge is approached (Brown et al., 2006).

Figure 3 also shows the measured soil profile along the centre-line of the trench before and after the test. The trench is shallow at the start of displacement and increases gradually during transition. It seems to have reached a steady-state depth when the trench is 500 mm along the box edge which corresponds to the skid tip being positioned at x ≈ 700 mm (the plough skids are approximately 200 mm in front of the share tip which cuts the trench). It takes approximately another 200 mm of displacement for the tow force to reach a steady-state condition. Due to gradual spoil heap formation in front of the share blade. The steady-state trench depth is 32 mm. Figure 4 shows a photograph of the soil sample after the test taken looking in the direction of plough movement. The transition zone can be observed at the bottom of the image, where the trench is shallower and the spoil heaps are smaller. The starting point for the skids is also visible near the bottom of Figure 4.

Reese and Grinstead (1986) suggested that the tow force (F) ,

$$F = C_w W + C_s \gamma D^3 \qquad (2)$$

where C_w and C_s were empirical coefficients, W was the buoyant plough weight, γ was the buoyant unit weight of the soil and D the trench depth. Brown et al. (2007) suggested that C_w = 0.482 and C_s ≈ 20 which differ to the values recommended by Cathie & Wintgens (2001). For the above values using γ = 15,000 N/m^3, W = 13.2 N and

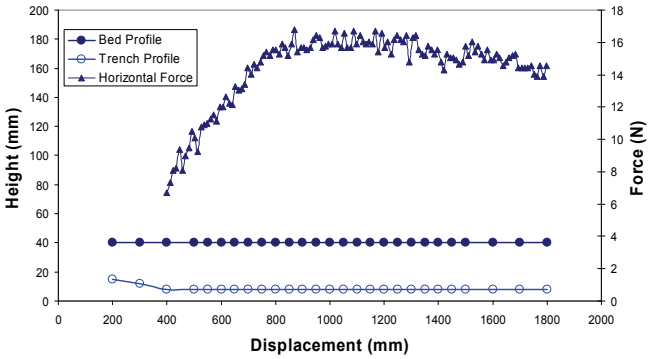

Fig. 3. Data from the flat soil test.

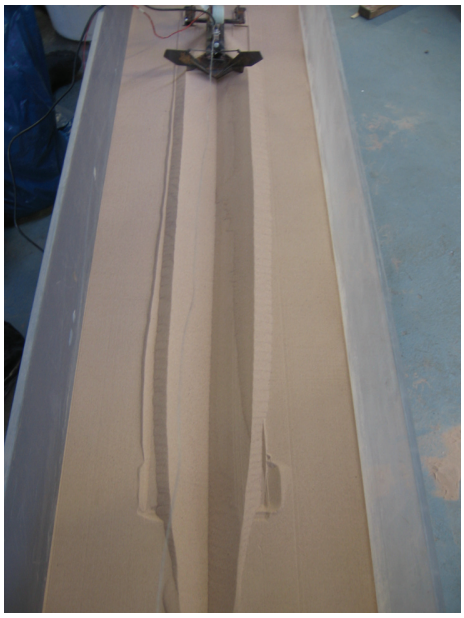

Fig. 4. Photograph taken at the conclusion of the flat bed plough test showing the ploughed trench and the spoil heaps.

D = 0.032 m, Eq. 2 suggests that F = 16.2 N. This is an excellent match with the 16 N measured.

Test 1_0.1. Wavelength, L = 1000 mm; h/L =0.1

The results of the test with a wavelength, L = 1000 mm and amplitude h/L = 0.1 are first shown in detail to explain the data that can be obtained during testing. This condition is of a sand wave as categorized by Gass et al. (1984) and has the longest wavelength investigated.

The tow force-displacement relationship and the soil profiles along the length of the trench are shown in Figure 4. The data set with solid squares shows the initial soil profile and shows the single wave from x = 500 mm to x = 1500 mm. The solid triangle data set shows the force-displacement relationship for this test. At the start of plough displacement, the forces are similar to those for a flat test with identical skid settings (also shown as crosses in Fig. 5) and most of transition is complete by x = 600-700 mm. However, the tow force then rises steeply with further displacement as the plough comes into contact with the sand wave. The peak load measured, F_{max} = 22.5 N is significantly higher than in the flat bed test (F = 12.5 N). The peak force occurs for a

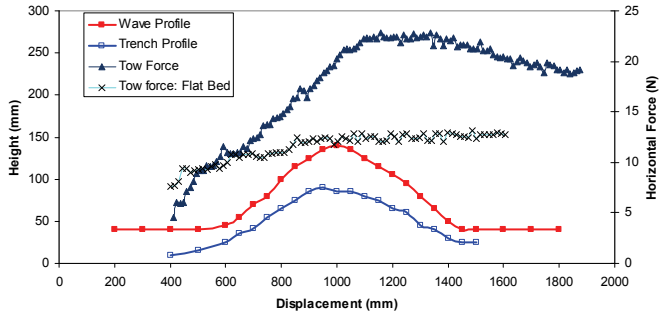

Fig. 5. Tow forces and trench profile for test 1_0.1 (L = 1000 mm; h/L = 0.1)

range of skid tip positions 1150 mm < x < 1350 mm and so occurs when the tip of the skid is 150 to 350 mm beyond the peak of the wave. Given that the tip of the skid is approximately 200 mm in front of the share tip, this suggests that peak force was measured when the share tip was at the peak of the sand wave.

Figure 5 shows the measured plough rotation (from the clinometer) and the trench depth (from the data shown in Fig. 4). The clinometer shows that the plough starts off with a negative rotation (i.e. the tip of the share is below the heel) before movement starts. Transition involves this rotation reducing as the plough share cuts further into the soil and the skids remain on the soil surface. On encountering the sand wave, the plough rotates to climb the wave and so the rotation becomes positive (aft-pitching). The maximum positive rotation of 12.5^o is reached almost exactly when x = 1000 mm (i.e. when the skid is at the peak of the wave) before the rotation angle decreases. It starts to become negative again (associated with moving down the wave) when x > 1312 mm, before reaching a negative peak (θ = -11.3^o) when $x \approx$ 1550 mm. This maximum point may coincide to the whole plough moving down the wave. Finally, rotation gradually reduces to about 2^o of forward pitch (-2^o) as the wave is left behind and the flat bed steady state condition is approached. For comparison, the maximum slope angle is 17.4^o in the steepest section of the sine wave.

Figure 6 also shows calculated rotations using the data from the trench and soil surface profile. The calculations make the assumption that the skids are on the original wave profile (at x) and the share is on the as-trenched profile (at x – 300 mm) and so:

$$\theta = \tan^{-1}\left(\frac{y_{surf}(x) - y_{trench}(x-300)}{300}\right) \qquad (3)$$

where y_{surf} is the surface vertical position and y_{trench} is a the vertical position of the base of the trench, both of which vary with position along the box (x).

The calculations show that rotation is reasonably well predicted by this method. However, errors in the method could come from three sources: (i) errors in measurement of the trench profile or surface soil profile. Note that the first one or two trench base measurements appear questionable in Fig. 5 which would explain the over-calculation of rotation when $x \approx$ 700 mm; (ii) From the assumption that the skids remain exactly at the soil surface. The skids may bury themselves a little during ploughing (e.g. Fig. 2); and (iii) because the final measured ('virtual') trench profile may not be the same as the trench depth when the plough share is cutting it because soil from the spoil heaps fall back after the plough passes to partly fill the trench.

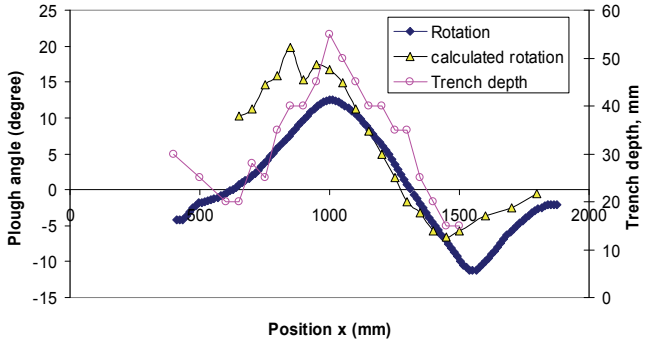

Fig. 6. Plough rotation and trench depth against position (test 1_0.1. L = 1000 mm; h/L = 0.1)

Finally, Figure 6 shows the calculated trench depth. The deepest trench occurs at the crest of the sand wave (i.e. at x = 1000 mm) where D = 55 mm. The peak load occurs for 1150 mm < x < 1350 mm (x is the position of the skid tips) which coincides closely with the share being at approximately the position of the wave crest (1000 mm).

Interestingly if D = 0.055 m is input to Eq. 2 with the parameters used for the flat test (C_s = 20, C_w = 0.48), F = 56.2 N which gives a 150% over-prediction of the measured force (22.5 N). This over-estimation occurs because although the depth at the tip is 0.055 m, the soil depth elsewhere along the plough is less because of the wave geometry and so less soil has to be moved by the plough. Another issue is that the cable pulling angle will vary as the plough traverses the sand wave and this may lead to a further change in tow force.

Figure 7 shows the measured soil height (relative to the base of the box) for four different cross-sections perpendicular to the plough axis. These positions correspond to the flat bed section (x = 500 mm), upslope (x = 750 mm), the wave crest (1000 mm) and then down-slope (1250 mm) (see Fig. 5). For all four positions, the trench angle (between the spoil heaps) varies from 28^o to 32^o agreeing approximately with the angle of repose of the soil and the share angle. Clearly, the depth of the trench (at z = 0 mm) relative to the horizontal far-field (i.e. at z = +-250 mm) varies with position as already plotted in Figure 6.

The size of the spoil heaps is also important as this indicates how much soil is available for backfilling and hence may dictate the achieved cover depth, H. At x = 500 mm and 1250 mm there is sufficient volume of spoil so that if it is assumed that the spoil at those positions is pushed back into the trench at the same position then a cover depth at least equal to D minus the pipeline diameter, d can be achieved (i.e. Cover depth, $H \geq D - d$). However, when the pipeline is going up the wave (x = 750 mm) or at the crest (x = 1000 mm), Figure 7 reveals that the spoil volume is too small to fill the trench. Volume calculations assuming a pipe diameter of 6 mm (equivalent to a 50th scale typical 0.3 m diameter pipe) and assuming that the volume of the soil does not change during backfilling (already at critical state), reveal final cover depths of 19.0 mm (at x = 750 mm) and 4.2 mm (at x = 1000 mm). Up-slope (x = 750 mm) the 19.0 mm achievable cover is a little smaller than the 23 mm from the calculation, $H = D - d$ and represents a cover depth of 0.8 m at full scale. Of most interest/concern is the spoil volume at the crest of the wave (at x = 1000 mm) which is very small compared to the trench depth. Here, the calculated 4.2 mm cover depth after backfilling represents a depth of only 0.21 m (i.e. H/d = 0.7) at full-scale equivalent. This reduced cover depth coincides almost exactly with the highest point of the trench base where it is likely any pipeline will be experiencing its highest uplift load due to thermal

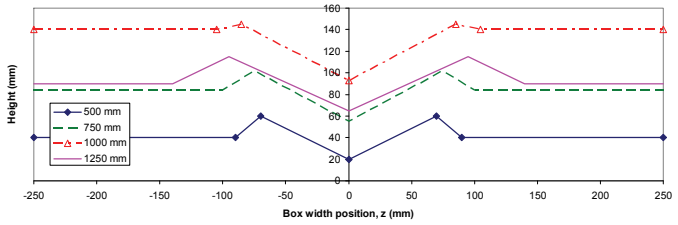

Fig. 7. Lateral trench profiles at different positions.

expansion. Consequently the lowest cover depth is achieved in exactly the place where most vertical restraint is required and so rock-dumping may be a requirement in such conditions.

Figure 8 shows a digital image captured of the soil conditions after ploughing. The small spoil heaps at the wave crest can be seen and these are a result mainly of the plough pushing the spoil heaps down the wave front during ploughing.

In summary, the maximum tow force increased significantly for the single wave and gave a trench profile which was in phase with the soil surface (i.e. the peaks and troughs of the waves and trench were coincident). However, the amplitude of the variation of the trench depth was not the same as that of the wave and so the trench depth was deeper near the wave crest (partially explaining the increase of tow force). However, there were very small spoil heaps in this section as it was pushed down-slope and so it would be difficult to backfill a pipeline. If this occurred in the field, the wave crest positions may prove critical and might require rock dumping to achieve appropriate buckling restraint.

Test 2_0.1. Wavelength, *L* = 500 mm; *h/L* =0.1.

The test with a wavelength, L = 500 mm and amplitude h/L = 0.1 corresponds to a mega-ripples (L = 25 m; h = 2.5 m) at full scale and shows the effect of reducing the wavelength for waves with the same wave amplitude to wavelength ratio (h/L).

Firstly, the tow force-displacement relationship and the soil profiles along the length of the trench are shown in Figure 9. The plotted wave profile (filled in squares on Fig. 9) shows the two waves which were

Fig. 8. Digital image of spoil heaps after test (L = 1000 mm, h/L = 0.1)

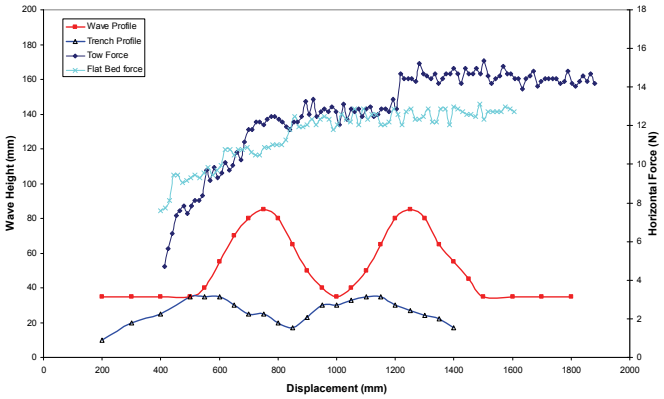

Fig. 9. Tow forces and trench profile for test 2_0.1 (L = 500 mm; h/L = 0.2)

situated in the middle of the test bed. Wave crests are situated at x = 750 mm and 1250 mm and the wave heights were 50 mm.

The trench profile data (Fig. 9) reveals a trench base that does not follow the wave crest as seen for the larger wavelength (Fig. 5). Instead, the trench base starts to rise as the plough encounters the upslope of the first skid, but then flattens out at $x \approx 600$ mm (when the skids start to encounter the down-slope of the first mega-ripple) before starting to fall again approaching the wave trough as the whole plough starts to descend the wave. The same process is repeated approximately for the second wave. The above response means that the sand waves and trench base are out of phase and there is a wide fluctuation in the trench depth achieved. In the trough between the two waves, there is almost no trench depth achieved although this might be partly due to flow of spoil heaps back into the trench as the plough rises over the second wave raising the trench depth height. The fact that the trench profile and wave profiles are out of phase is advantageous as it means that there are relatively large trench depths at the points where the trench base is at its highest.

The tow force data shows little increase compared to the flat bed test especially for the first wave encountered and surprisingly little fluctuation in load as the plough goes over/through each wave. There is an approximately 16% increase in tow force when the second wave is encountered.

Test 3_0.1. Wavelength, *L* = 300 mm; *h/L* =0.1

A test with a shorter wavelength mega-ripple is presented next (Fig. 10). This time, the wavelength is shorter than the plough length and the plough share seems to travel almost horizontally in the zone of mega-ripples leaving a fairly level trench (open squares in Fig. 10). Consequently, the trench depth fluctuated as also observed in test 2_0.1.

Despite the fluctuations in trench depth, the tow force appears almost constant through the mega-ripple zone and approximately the same as in the flat bed test (12.5 N). The average measured trench depth in the test is 29 mm which would lead to a predicted tow force, F = 13.7 N using equation 2 and the previously selected parameters, suggesting that the waves have surprisingly little effect on the tow force.

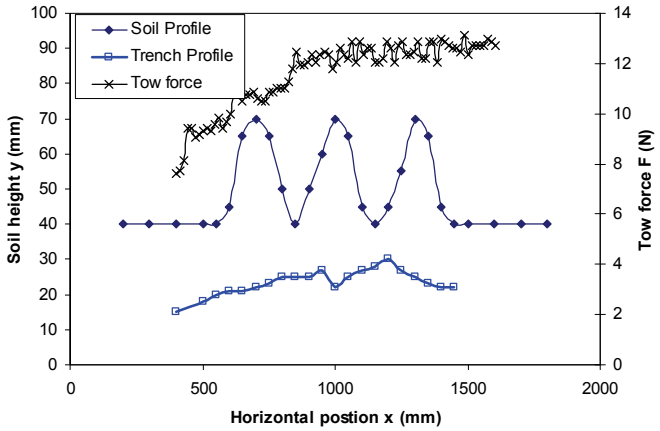

Fig. 10. Tow force and trench profile data for test 3_0.1 (L = 300 mm; h/L = 0.1).

Test 2_0.2. Wavelength, L = 500 mm; h/L =0.2.

Finally the results from a test with a wavelength, L = 500 mm and amplitude h/L = 0.2 is shown in Figure 11. This soil surface shape corresponded to high amplitude mega-ripples (L = 25 m; h = 5 m) at full-scale and can be compared to the results from test 2_0.1.

As in test 2_0.1, the trench profile data (Fig. 11) reveals a trench base that does not follow the mega-ripples; the sand waves and trench base are out of phase and there is a wide fluctuation in the trench depth achieved. Thus the kinematic response of the plough for the two tests with different amplitude waves appears similar.

However, the tow force data shows a large increase compared to the flat bed test and significant fluctuations as the plough goes over/through each wave. This is very different to the response seen in the lower amplitude test (test 2_0.1; Fig. 9). The maximum tow force measured is 32 N, a 146 % increase compared to the flat bed test (≈ 13 N). In the field, this type of load increases will at best produce a large reduction of plough velocity and at worst, totally prevent plough movement if the vessel tow capacity is insufficient.

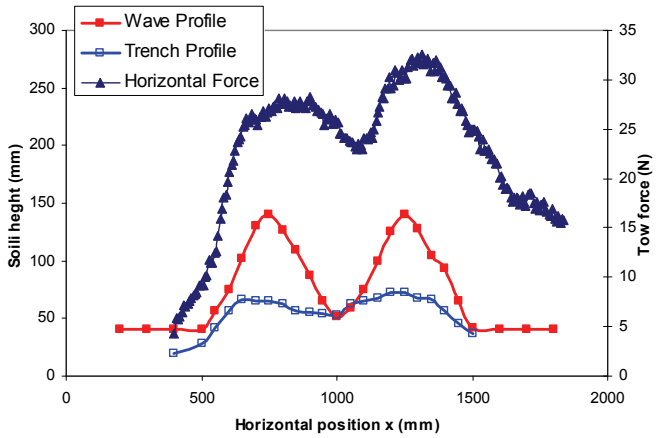

Fig. 11. Tow forces and trench profile for test 2_0.2 (L = 500 mm; h/L = 0.2)

DISCUSSION

Results from four example tests from a larger data set have been discussed. These showed that plough performance varied particularly with the wavelength of the sand waves/mega-ripples, but also with the amplitude. Perhaps, the two extremes of performance were observed in test 1_0.1 and test 3_0.1. For the single, long wavelength sand wave (test 1_0.1), the plough generally followed the wave and tow forces were increased significantly. The practical issue here was the cover depths achievable at the wave crest and the implication of increased tow force. For the shorter wavelength mega-ripple (test 3_0.1), the trench profile fluctuated very little compared to the wave height (and so the trench depth fluctuated widely) and the tow forces seemed to reflect the average trench depth in the mega-ripple zone and were not significantly increased compared to the flat bed condition. However, the intermediate, high amplitude wavelength mega-ripple test revealed large increases in tow forces and suggested that prediction of the increases in tow force in zones of mega-ripples is also important.

CONCLUSIONS

A series of 1/50th scale model tests have been conducted to investigate the performance of pipeline ploughs in areas of mega-ripples and sand waves. The tests revealed the following:

1. For long wavelength sand waves compared to the plough length, the plough approximately followed the soil surface. An increase in tow force resulted together with a fluctuating trench base. The trench depth fluctuated along the wavelength a little, but perhaps more importantly the size of the spoil heaps available for backfilling fluctuated significantly, with almost no spoil being available at the wave crest.
2. For short wavelength mega-ripples, the plough share did not follow the soil surface but moved horizontally through the waves leaving an almost level trench depth. For the waves with amplitude h/L =0.1, there was a surprisingly small increase in tow force.
3. For megaripples with intermediate wavelength, an intermediate response was observed with a fluctuating trench depth which was out of phase with the original sand waves. In addition, a test with large amplitude waves revealed significant increases in tow force.
4. Further testing is required to reveal more about plough kinematics and tow force changes in regions of sand-waves and mega-ripples. However, this paper has revealed new mechanisms and considerations for practice.

ACKNOWLEDGEMENTS

The third author is supported jointly by the EPSRC and CTC Marine Projects Ltd. We are grateful for the support.

REFERENCES

Bransby, M.F., Yun, G.J., Morrow, D.R. & Brunning, P. (2005). *"The performance of pipeline ploughs in layered soils."* Frontiers in Offshore Geotechnics: ISFOG 2005, Gourvenec & Cassidy (Eds), pp 597-606.

Brown, M.J, Bransby, M.F & Simon-Soberon, F. "*The characteristics of a model pipeline plough"*. Proc. International Conference on

Physical Modelling in Geotechnics, Hong Kong, August 2006, pp 709-714.

Cathie, D. N. & Wintgens, J. F. (2001) "*Pipeline Trenching Using Plows: Performance and Geotechnical Hazards*." Proc. Thirty-third Annual Offshore Technology Conf., Houston (13145) April/May 2001, pp 1-14

Gass, IG and Course Team (1984). *Oceanography: Sediments*. The Open University.

Lauder, K.D., Bransby, M.F., Brown, M.J., Pyrah, J., Steward, J & Morgan, N. (2008) "*Experimental testing of the performance of pipeline ploughs,"* Proc. Eighteenth (2008) Int. Offshore and Polar Engineering Conf. Vancouver, Canada, July 6-11 2008.

Morrow, D. R. and Larkin, P. D. (2007) "The challenges of pipeline burrial" *Proc. Seventeenth (2007) Int. Offshore and Polar Engineering Conf.* Lisbon, Portugal, July 1-6 2007.

Palmer, A. C., Kenny, J. P., Perera, M. R. & Reece A. R. (1979). "Design and operation of an underwater pipeline trenching plough," *Géotechnique,* Vol 29, No 3, pp 305-322.

Palmer, A.C. (1999) "Speed effects in cutting and ploughing," *Géotechnique*, Vol 49, No 3, pp 285-294.

Reece, A. R. and Grinsted, T. W. (1986). "*Soil Mechanics of Submarine Ploughs*" Proc. Eighteenth Annual Offshore Technology Conf., Houston (5341) May 1986, pp 453-461